



HAL
open science

Early transition in microchannels under EDL effect

Sedat F. Tardu

► **To cite this version:**

Sedat F. Tardu. Early transition in microchannels under EDL effect. SPIE International Symposium: Micromachining and Microfabrication, 2004, San José, United States. 10.1117/12.523603 . hal-00262230

HAL Id: hal-00262230

<https://hal.science/hal-00262230>

Submitted on 3 Apr 2020

HAL is a multi-disciplinary open access archive for the deposit and dissemination of scientific research documents, whether they are published or not. The documents may come from teaching and research institutions in France or abroad, or from public or private research centers.

L'archive ouverte pluridisciplinaire **HAL**, est destinée au dépôt et à la diffusion de documents scientifiques de niveau recherche, publiés ou non, émanant des établissements d'enseignement et de recherche français ou étrangers, des laboratoires publics ou privés.



Distributed under a Creative Commons Attribution 4.0 International License

EARLY TRANSITION IN MICROCHANNELS UNDER EDL EFFECT

Sedat Tardu

Laboratoire des Ecoulements Géophysiques et Industriels
LEGI BP 53 X Grenoble Cedex- France

ABSTRACT

The effect of the electric double layer (EDL) on the linear stability of Poiseuille planar channel flow is reported. It is shown that the EDL destabilises the linear modes, and that the critical Reynolds number decreases significantly when the thickness of the double layer becomes comparable with the height of the channel. The planar macro scale Poiseuille flow is metastable, and the inflexional EDL instability may further decrease the macro-transitional Reynolds number. There is a good correspondence between the estimated transitional Reynolds numbers and some experiments, showing that early transition is plausible in microchannels under some conditions.

1. INTRODUCTION

The characteristics of gas flows in microchannels can adequately be modelled by slip velocity and temperature jump related to first or second order models as a function of the Knudsen number, at least in the rarefied regime. Such molecular effects are difficult to model in micro-liquid flows. Yet, estimations obtained from some molecular models indicate that the discontinuous boundary conditions could only hold for microchannels of hydraulic diameters smaller than few microns (Gad-el-Hak, 1999, Tardu, 2003). The interfacial effects (wall/liquid) are presumably mostly responsible for the deviations observed from the classical macro-theory, in larger microchannels. One of the micro-effects that may play an important role is the electric double layer (EDL) at the solid/liquid interface. The electrostatic charges present on the solid surface attract the counterions to establish an electrical field.

In the compact layer next to the wall the ions are immobile. In the diffuse EDL layer however, the ions are less affected by the electrical field and can move. Under the effect of an imposed pressure gradient, the accumulation of the mobile ions downstream sets up an electrical field that induces a streamwise external force. In macroscale flows, these effects are negligible, as well as the thickness of the EDL is very small compared to the height of the channel. In microflows, in return, the EDL play a rather significant role. Well-controlled recent experiments have clearly confirmed that it can explain the behaviour of the Poiseuille number in laminar regime, providing that the liquid contains a very small amount of ions (Ren et al. 2001). Kulinsky et al. (1999) reported an increase of 70% of the friction factor under the EDL effect in planar channels of 4 μm heights with distilled water. Large thickness of the diffuse EDL layer of about 1 μm or more have been reported in these experiments.

There is a curious phenomena encountered in some experiments showing that there is an early transition in microchannel flows. Weng and Peng (1994) noticed that the transition occurred at $Re < 150$ in microchannels 0.2-0.8 mm wide and 0.7 mm deep, which is significantly smaller than 400 corresponding to macro scale flows (The Reynolds number through this paper is based on the centreline velocity and half height of the channel. Thus 400 correspond to a Reynolds number based on hydraulic diameter and cross section average velocity of 2000). A transitional number of about 250 has also been reported in the experiments conducted in 1mm wide trapezoidal microchannels with channel depths ranging between 79 and 325 μm (Rahman and Gui, 1993 a and b, Gui and Scaringe 1995). The micro tubes experiments of Mala and Li (1999) indicate that there is an early transition from laminar to turbulent flows for $Re > 56-170$. These effects may be attributed to the roughness that may both influence the transition in the entry region, or directly affect the flow behaviour through an implied roughness-viscosity (Weilin et al., 2000). Yet, direct interfacial effects may also play a role in presumed early transition.

The stability mechanism in planar channel flows is mainly non-linear and the secondary instabilities cause the flow to bifurcate before the critical Reynolds number of linear modes. That depends on the behaviour of the time space

development of the perturbations near the critical Re and wave numbers. The main aim of this study is to investigate directly the EDL effect on the linear stability of planar channel flow, and estimate indirectly the resulting transitional Reynolds numbers. It is asked whether electrokinetic effects on liquid flows may cause the early transition or not and whether the linear stability EDL flow characteristics may explain the small transitional Reynolds numbers encountered in studies quoted to before.

2. PHYSICAL ASPECTS OF ELECTRIC DOUBLE LAYER

Most solid surfaces have an electric surface potential when brought with an electrolyte. The most common mechanism for the charging of surface layers in microfluidics is the deprotonation of surface groups on surfaces such as silica, glass, acrylic and polyester (Hunter, 1981, Sharp et al., 2002). The electrostatic charges present on the solid surface attract the counterions to establish an electrical field (Fig. 1). In the compact layer next to the wall and less than 1 nm thick the ions are immobile. In the diffuse EDL layer however, the ions are less affected by the electrical field and can move. The counterion concentration near the wall is larger than in the bulk of the fluid. That results in a net charge density in a unit volume resulting from the concentration difference between cations and anions, according to the Boltzmann equation. The electrostatic potential at any point near the surface, provided that it is small compared to the energy of ions, may be obtained by a linear approximation of the Poisson-Boltzmann equation. Its value at the wall can be related to the Zeta potential between the compact layer and diffuse layer, when the EDLs near the opposite walls do not overlap. The Zeta potential is a property of the solid-liquid pair and can be determined experimentally. The imposed pressure gradient accumulates the mobile ions downstream and sets up an electrical field whose potential is called the streaming or electrokinetic potential. The streaming potential and the net charge density induces a streamwise external force. In the steady state, the streaming current due to the transport of charges is in equilibrium with the conduction current in the opposite direction. That allows the determination of the streaming potential and of the velocity profiles under the EDL effect.

3. EQUATIONS GOVERNING 2D CHANNEL FLOW UNDER THE EDL EFFECT

We suppose constant properties (viscosity and permittivity). The effects of finite ion size and gradients of the dielectric strength and of the viscosity are neglected. These hypotheses are not contradictory with the fact that we mainly deal with very dilute solutions for which the equilibrium Boltzmann distribution is applicable. The velocity profile under the electrokinetic EDL effect obtained by Mala et al (1997) can be put in non-dimensional form as:

$$u = 1 - y^2 - 4 \frac{I_1 - I_2}{\frac{\kappa^2 \sinh \kappa}{\bar{\zeta}^2 G} + 4 \left(I_3 - \frac{I_4}{\sinh \kappa} \right)} \left\{ 1 - \left| \frac{\sinh \kappa y}{\sinh \kappa} \right| \right\} \quad (1)$$

where, the scaling velocity is the centerline velocity of the Poiseuille component, i.e. $-\frac{a^2 dp/dx}{2\mu}$ and the scaling

length is the half channel height a . There are several parameters in this equation, for instance $G = \frac{(n_0 z e a)^2}{\lambda_0 \mu}$, with

n_0 standing for the ionic number concentration, z for the valence of positive or negative ions, e for the electron charge λ_0 the electric conductivity of the fluid, and μ for its dynamic viscosity. One of the most important quantities involving in (1) is the non dimensional Debye-Huckel parameter

$$\kappa = a k = a \left(2 n_0 e^2 / \varepsilon \varepsilon_0 k_b T \right)^{1/2} \quad (2)$$

with ε and ε_0 being respectively the dielectric constant of the medium and the permittivity of vacuum, k_b the Boltzmann constant and T the absolute temperature. The characteristic EDL thickness is $1/k$. The non-dimensional

Zeta potential reads for $\bar{\zeta} = \frac{z e \zeta}{k_b T}$. The quantities I in (1) are given by:

$$I_1 = I_3 = \frac{\cosh \kappa - 1}{\kappa}, I_4 = \frac{\sinh \kappa \cosh \kappa}{2\kappa} - \frac{1}{2}$$

$$I_2 = \left(\frac{1}{\kappa} + \frac{2}{\kappa^3} \right) \cosh \kappa - \frac{2}{\kappa^2} \sinh \kappa - \frac{2}{\kappa^3}, \quad (3)$$

It is seen that the velocity profile can be decomposed into a macro Poiseuille component plus an EDL effect component. A closer inspection of (1) allows expressing the later in another close form as:

$$u_{EDL} = -4 \frac{I_1 - I_2}{\frac{\lambda_0 \mu \sinh \kappa}{\bar{\zeta}^2} + 4 \left(I_3 - \frac{I_4}{\sinh \kappa} \right)} \left\{ 1 - \left| \frac{\sinh \kappa y}{\sinh \kappa} \right| \right\} \quad (4)$$

The parameter $\lambda_0 \mu$ is the non-dimensional electrical conductivity times the dynamic viscosity of the fluid. It can be seen that the scaling parameter for $\lambda_0 \mu$ is the square of the scaling charge density times the scaling length, i.e. $(\rho_S / k)^2$ leading to:

$$\lambda_0 \mu = \frac{\lambda_0 \mu}{(n_0 \varepsilon \varepsilon_0 k_b T / 2)} \quad (5)$$

There are three parameters governing the EDL effect, namely

$$u_{EDL} = u_{EDL}(\kappa, \bar{\zeta}, \lambda_0 \mu) \quad (6)$$

Gradients of the dielectric strength, viscosity and conductivity should be incorporated in more realistic models. Yet, these effects are presumably negligible in significantly dilute solutions, such as deionized ultra filtered water (DIUFW) and pure organic liquids.

The main EDL effects may be summarized as follows:

- An increase of the friction constant and apparent viscosity.
- A decrease of the Nusselt number.

These effects are persistent yet not significantly important at least for large values of κ . The apparent viscosity increases for example by a factor of nearly 3 at $\kappa=2$, but the EDL effect on the wall shear stress disappears quickly when $\kappa \geq 10$ (Mala et al., 1997). The Nusselt number decreases by nearly 40% at $\kappa=5$, and less than 5 % at $\kappa=50$ (Tardu, 2003).

4. INFLEXIONAL INVISCID INSTABILITY

The EDL effect is undoubtedly significant for small values of κ for the liquids containing a very small number of due for example to impurities. In such situations the thickness of the diffuse layer may reach several micrometers. Fig. 2a compares the velocity profile of an “EDL flow” with the conventional Poiseuille flow, when $\kappa=41$, $G=12720$ and $\bar{\zeta}=2.1254$. This case corresponds to the flow of an *infinitely* diluted aqueous solution ($n_0=3.764 \times 10^{19} m^{-3}$) through a microchannel of height $100 \mu m$ subjected to a Zeta potential of 50 mV. The Debye length is $1.2 \mu m$, which is close to the value corresponding to the de-ionized ultra-filtered water experiments of Ren et al. (2002). The first impression one has from Fig.2a is the close similarity between the EDL and Poiseuille profiles with a decrease of the centreline velocity typical to the EDL flows. The increase of the friction constant is only 16 % in this situation. The important difference however is the presence of an inflexional point at $y \approx \frac{1}{\kappa} \arcsin h \left\{ -\frac{2}{r\kappa^2} \sinh(\kappa) \right\}$ in the EDL profile where r is the ratio of the EDL and Poiseuille flow centreline velocities. This makes the flow inviscidly unstable, according to the Fjortoft’s criteria (Fig. 2b). The inviscid instability does not imply instability directly in wall flows and an Orr-Sommerfeld analysis is necessary.

5. STABILITY ANALYSIS

The linear hydrodynamic stability under the EDL effect is studied through classical methods. The Orr-Sommerfeld equation is solved by a Galerkin-like procedure (Von Kerczek, 1982). The normal mode solutions of the disturbance equation are:

$$(u, v, p) = R(\alpha, \alpha, \alpha) \exp(i\alpha x) \quad (7)$$

R is the real part, α is the dimensionless wave-number of the disturbance and x is the streamwise coordinate.

Introducing the stream function:

$$\psi(x, y, t) = \phi(y, t) \exp(i\alpha x) \quad (8)$$

the Orr-Sommerfeld equation takes the form:

$$\frac{\partial}{\partial t} L\phi = \frac{1}{Re} L^2 \phi - i\alpha \left(u L\phi - \frac{d^2 u}{dy^2} \phi \right) \quad (9)$$

with the boundary conditions $\phi = \frac{\partial \phi}{\partial y} = 0$ at $y = \pm 1$. The operator L is $L \equiv \frac{\partial^2}{\partial y^2} - \alpha^2$. The stream function is expanded in a Chebyshev polynomial series:

$$\phi(y, t) = \sum_{n=1}^N a_n(t) T_{2n-2}(y) \quad (10)$$

where $T_m(y) = \cos(m \cos^{-1} y)$ denotes the Chebyshev polynomials of the first kind. We took $N=256$ through this study. Eq. 9 takes the form:

$$\mathbf{Q} \frac{d\mathbf{a}}{dt} = (\mathbf{P} - i\alpha \mathbf{J}) \cdot \mathbf{a} \quad (11)$$

and the matrices are determined by making use of the τ -method described by Orszag (1971). The last equation can be written as:

$$\frac{d\mathbf{b}}{dt} = \mathbf{D} \cdot \mathbf{b} \quad (12)$$

by introducing \mathbf{B} the matrix that diagonalizes $\mathbf{Q}^{-1} \cdot (\mathbf{P} - i\alpha \mathbf{J})$, $\mathbf{b} = \mathbf{B}^{-1} \cdot \mathbf{a}$ and the diagonal matrix $\mathbf{D} = \lambda_i \delta_{ij} = \mathbf{B}^{-1} \cdot \mathbf{Q}^{-1} \cdot (\mathbf{P} - i\alpha \mathbf{J}) \cdot \mathbf{B}$. The eigenvalues are denoted by λ_i and the flow is unstable when $R(\lambda_i) > 0$. The disturbances with symmetric streamfunctions are considered only. The method gave very close results to Grosch and Salwen (1968) who used different sets of expansion functions.

6. RESULTS

Fig.2 shows the neutral curve corresponding to the microchannel-flow with the parameters given below, together with a ‘‘macro’’ Poiseuille flow (i.e. $\bar{\zeta} = 0$ or $\kappa \rightarrow \infty$). It is clearly seen that the critical Reynolds number decreases by a factor nearly equal to 2 under the effect of EDL: the critical wave and Reynolds numbers of the microflow are respectively $\alpha_c = 1.10$ and $Re_c = 3190$ to be compared with $\alpha_c = 1.02$ and $Re_c = 5772$ of the conventional Poiseuille flow. Due to its inviscid inflexional instability (unstable for $Re \rightarrow \infty$ for a given α), the band of unstable wave numbers of the EDL-microflow is significantly larger compared with the Poiseuille-macroflow. The destabilizing EDL effect disappears quickly when the height of the channel is increased by a factor of 4 (400 μm) (triangle in Fig. 2 corresponding to $\kappa = 163$). This goes in the same line as previous experimental results showing the lack of micro-effects for the microchannels of height larger than typically 100 μm . For smaller values of κ , in return, the effect of the interfacial effects caused by EDL on the transition may be much more severe. For instance, the critical Reynolds number decreases up to $Re_c = 1042$ for a channel with a 40 μm separation distance subject to the same conditions (the square in Fig. 2 with $\kappa = 16$), and to a value as small as $Re_c = 496$ when $\kappa = 8$. It is clear that one of the most significant effect of EDL is the decrease of the critical Reynolds number, rather than the increase in friction coefficient or the apparent

viscosity. For $\kappa = 40$, the friction factor increases by some 7%, but the critical Reynolds number DECREASES by 100%.

Fig. 3 shows the spectrum of eigenvalues as a function of Re for a single fixed wave-number $\alpha=1$ and $\kappa=16$. Only the first three eigenvalues corresponding to the complex wave speed $c = -\lambda / i\alpha$ are shown for the sake of clarity. The modes are ordered in such a way that ascending values correspond to descending values of $\text{Im}\{c\}$, i.e. of $R\{\lambda\}$. Remind that the flow is stable (unstable) for $R\{\lambda\} < 0$ (> 0). The Re number was varied from 300 to $20 \cdot 10^3$. The curves corresponding to Poiseuille and EDL-flows are denoted respectively by P-i and E-i. It is seen in Fig.3 that only the first mode has a different $\text{Im}\{c\}$ under the EDL effect and that the imaginary parts of higher modes collapse entirely with those of the macro scale flow. Note however that $\text{Im}\{c_{1-EDL}\}$ is much more positive than $\text{Im}\{c_{1-Poiseuille}\}$ showing the strong destabilizing effect of the EDL. The EDL modes are slower than the Poiseuille ones, in the sense that $R\{\lambda_{EDL}\}$ is smaller than $2/3$ which is the average velocity of the channel, while the modes 2 and 3 of macro scale flow are clearly fast modes (their phase speed is close to the centerline velocity).

We have shown that, the EDL velocity component depends on the group of parameter $G\bar{\zeta}^2$ for a given Debye-Hückel parameter κ . The parameter G can be expressed as a function of the non-dimensional conductivity and viscosity product as $G = \frac{\kappa^2}{\lambda_0 \mu}$, showing that G varies like the inverse of $\bar{\lambda}_0 \mu = \frac{\lambda_0 \mu}{(n_0 \varepsilon \varepsilon_0 k_b T/2)}$ for fixed κ . Thus G increases with decreasing conductivity and/or viscosity.

To each couple $(\kappa, G\bar{\zeta}^2)$ corresponds a different set of the critical wave and Reynolds numbers (α_c, Re_c) . It is difficult to illustrate the interdependency of Re_c via $G\bar{\zeta}^2$, since α_c changes continuously as $G\bar{\zeta}^2$ varies. We fixed the wave number at its macro-scale flow critical value $\alpha_c = 1.02$ to give a general tendency and extract clear information.

Figure 4 shows the distribution of Re_c versus $G\bar{\zeta}^2$ for four different values of κ . Consider first the results corresponding to the smallest value $\kappa = 8$. The effect of the inviscid instability is so important in this case that the critical Reynolds number changes rapidly even for insignificantly small values of the Zeta potential. For instance Re_c varies by 25% with $Re_c = 4300$, already at $G\bar{\zeta}^2 = 10$. That would correspond to a Zeta potential of only 0.66 mV for the reference case. Increasing the Zeta potential by 10 from this value decreases Re_c by nearly 3. There is a range of $G\bar{\zeta}^2$ in which the critical Reynolds number decreases sharply before reaching a plateau region wherein Re_c is close to the critical number deduced from the neutral curves. This range varies with κ (Table 1) and it is about two decades large. The lower and upper limits of the $G\bar{\zeta}^2$ range increase with κ . It is clear both from both Fig. 4 and Table 1 that Re_c is more sensitive to $G\bar{\zeta}^2$ when the Debye-Hückel parameter is small enough, say for $\kappa \leq 40$. The first and main condition to expect significant EDL effects on hydrodynamic linear stability is to deal with liquids of low ionic concentration. The second condition requires large enough $G\bar{\zeta}^2$ value. This is fulfilled by low conductivity, which is generally associated with wall/liquids interactions that lead to high Zeta potential $\bar{\zeta}$. The second condition is less critical than the first. To show this, consider a median value of $\kappa = 20$. Fig. 4 shows that Re_c decreases by a factor 6 already at $G\bar{\zeta}^2 = 10^3$, corresponding for example to $G = 250$ and $\bar{\zeta} = 2$, that is, a liquid which is 50 times more conductive than the reference case.

7. DISCUSSION AND CONCLUSION

We have shown that EDL affects considerably the linear hydrodynamic stability of micro-channel flows under some specific conditions. The key question: Is this effect can experimentally verified, and explain early transition reported so far in some investigations?

To give preliminary answers to these questions and discuss related phenomena, we have first to note that the hydrodynamic linear stability and transition mechanisms are different in plane Poiseuille flows. What we are interested in from an applications point of view is indeed the transitional Reynolds number Re_t related but not strictly equals to Re_c .

According to Orszag and Potera (1983), the instability process of wall bounded macro-scale shear flows involves in three steps:

- 1- primary (linear) instability of the basic shear flow;
- 2- nonlinear saturation of the primary instability and formation of a secondary flow;
- 3- secondary instability, which is the linear stability of the secondary flow.

The first step gives $Re_c = 5772$ for macro-scale plane Poiseuille flows, but transitional Reynolds numbers as low as $Re_t = 400 - 1000$ have been reported in experiments. This is because the second step results in a Landau type mechanism leading to subcritical instability or the metastability: the instability occurs with finite amplitude when all infinitesimal disturbances are stable at a significantly lower critical value compared to Re_c (Drazin and Reid W.H., 1981). The secondary instability (step 3) is three-dimensional. The quasi-steady nonlinear analysis conducted by Orszag and Patera (1983) suggests a critical Reynolds number for the secondary instability of about $R \cong 400$. The direct numerical simulations they conducted have shown that three-dimensional disturbances decay for $R < 1000$, but 1000 can not be taken as a precise number, because the three dimensional instability requires that a threshold two-dimensional amplitude be achieved. The experiments indicate that the ratio of the transitional Reynolds number to the critical Reynolds number of the primary instability is about $r = \frac{Re_t}{Re_c} \approx \frac{750}{5772} \approx \frac{1}{8}$ (Schlichting, 1975) but this is not an exact universal value either.

There are some arguments suggesting that the EDL can reinforce the subcritical nature of macro Poiseuille flow through the non-linear saturation of the primary instability (step 2). Stuart (1960) has shown that there are three main mechanisms generating the subcritical equilibrium state. The first mechanism is the distortion of the mean motion and prevents the subcritical instability. This effect is proportional to $Re_c \alpha_c^2$ which is significantly small in EDL flow. The second mechanism is the wall normal distortion of the fundamental and it is inversely proportional to Re_c . EDL enhances directly the subcritical state through the second mechanism and retards the preventing first one. Simple arguments can not be given for the third process involving in the generation of the harmonic of the fundamental and a detailed analysis is necessary.

One of the simple explanations of the secondary instability (step 3) is the creation of local inflexional streamwise profiles with strong shear susceptible to inviscid instability (Utah, 1974, Orszag and Patera, 1982). The basic flow in EDL is already inflexional. Interactions of the first and second steps in the process may lead to significantly smaller transitional Reynolds numbers in the presence of EDL. The reasonable conclusion of these arguments is that the EDL flow is subcritical and the ratio of transitional to critical Reynolds numbers $r = \frac{Re_t}{Re_c} \leq \frac{1}{8}$.

We show in Fig.5 the estimated transitional Reynolds as a function of κ . We took the same ratio $r = \frac{Re_t}{Re_c} = \frac{1}{8}$ as in macro-scale flow, although significantly smaller r is expected under EDL effect. The open circles in Fig.5 correspond to the reference case. A second case, shown by bold circles is also introduced: we considered a liquid with the same parameters as the first reference case but which is 11.5 times less conductive, leading to $G\bar{\zeta}^2 = 5000$. The aim of Fig.5 has to be clarified. It is somewhat difficult to reach high Reynolds numbers in microchannels, because high pressure is then necessary and the channels may break. The present study is parametrical and one may, of course, always consider Debye lengths larger than $1 \mu m$, thus higher channels compared with the numerical examples given before. The transition may be easily determined by classical Re -pressure gradient curves or local wall shear stress measurements with micro-sensors of MEMS type. Fig. 5 shows that the expected transitional Reynolds numbers are within the range of experimental possibilities. We need a

Debye length to express data in terms of $Re - \kappa$ distribution. We took $\frac{1}{k} = 1.2 \mu m$ to be consistent. We report micro-channel data but also micro tubes data of Mala and Li (1999). It has to be recalled here that Hagen-Poiseuille flow is linearly stable, and some aspects of the transition in pipe flows can be explained only by secondary instabilities. That does not matter for the qualitative comparison made here and in the lack of well controlled investigations. It is seen in Fig.5 that the experimental Reynolds numbers are larger than Re_t , allowing to conclude that experimental verification of the present study is plausible, providing that some precise conditions are fulfilled as we will precise later.

Early transition in micro-channel flows has been reported in several experimental studies as we already indicated in the introduction. There are two data points related to transition in Fig.5. The first is from Mala and Li (1999) who indicated $Re_t \approx 300$ in micro-tubes with hydraulic diameters $D_h = 130 \mu m$. The bold square is the second point: the profiles at $D_h = 142 \mu m$ of Qu et al. (2000, their Fig. 8b, p.362) obtained in trapezoidal silicon microchannels suggest a transitional number of 400. There is a satisfactory agreement between the estimated transitional numbers and the experiments in Fig. 5, but that may be just coincidental. Controlled experiments in a way similar to those reported by Ren et al. (2002) have to be conducted. That may be achieved for instance by keeping the same channel with the same roughness distribution, and changing the ionic concentration of the liquid. Somewhat unfortunately, the maximum Debye length in Ren et al. experiments is four times smaller than the reference case taken here. Ren et al. (2001) and Sze et al. (2003) have measured the Zeta potential ($\zeta = 245 mV$), Debye length ($\frac{1}{k} = 0.305 \mu m$) and the bulk conductivity ($\lambda_0 = 1.053 \times 10^{-4} S/m$) in microchannels of height varying from $14.1 \mu m$ to $40.5 \mu m$. Note that the conductivity is 1.3×10^3 times larger than the reference case. The Zeta potential is too high for the linearization of the Poisson equation. The full equation has to be resolved, and the present estimation is therefore only qualitatively valid and the fact that the channels cross-section shape, in particular the corners have important contribution to the EDL field have also to be considered (Yang and Li., 1997, 1998). With these restrictions in mind, one has $\kappa = 23.6$ and $G\bar{\zeta}^2 = 500$ for the $14.1 \mu m$ height channel in Ren et al.'s experiments. Up to 20% higher flow resistance is found. The transitional Reynolds number decreases by some 63 %, with $Re_t \approx 270$. There is a significant effect on the transition, but the resulting Re_t is too high to be experimentally reached in such a small device. If, instead of $\frac{1}{k} = 0.305 \mu m$ the Debye length was $1 \mu m$ in Ren et al.'s experiments, one would have a 30% decrease in Re_t , with $Re_t \approx 500$ in their $40.5 \mu m$ width channel, with all other parameters being same. This is closer to experimental reality. This example illustrates the importance of large Debye lengths to reach early transition in microchannels.

In Weng and Peng (1994) the value of κ is presumably larger than 120 for microchannels of hydraulic diameters larger than $150 \mu m$ these authors investigated. Although their experiments have been conducted with distilled water (so that roughly $1/k = 1 \mu m$) the low transitional Reynolds numbers of about 300 they report can not be explained by the EDL effect. Strong effect of roughness in the inlet region is suspected in these experiments.

To conclude, the electro-viscous effects modify the linear stability characteristics of micro-channel flows. Three main conditions are required for a significant alteration of the critical Reynolds number:

i- The non-dimensional Debye-Hückel parameter should be smaller with typically $\kappa \leq 40$. There is no effect on stability for liquids with high ionic concentration and/or mini channels.

ii- Large enough Zeta potential and liquids with low conductivity/viscosity leading to $G\bar{\zeta}^2 \geq 5000$ for $\frac{1}{k} \approx 1 \mu m$ are necessary. This condition is less critical than the first one. With $\frac{1}{k} = 2 \mu m$, that is a Debye length which is just two times larger than the reference case, the critical Reynolds number decreases by nearly 80 % in a $32 \mu m$ width channel at $G\bar{\zeta}^2$ as small as $G\bar{\zeta}^2 = 100$.

The non-linear stability analysis of EDL flow is interesting both from a fundamental and application point of view. There are some reasonable arguments indicating that the EDL reinforce the subcritical nature and

secondary instabilities of micro-channel flows, but detailed analysis is necessary for confirmation. We are currently investigating this aspect.

Early transition in microchannels can have interesting applications for enhancement of mixing together with heat and mass transfer processes. A simple estimation shows that the ratio of the Nusselt numbers in EDL and macroscale flow is roughly inversely proportional to the ratio of the transitional Reynolds numbers. A decrease of Re_t by a factor f implies therefore an enhancement of the heat transfer by the same f in some giving working conditions.

Fully developed turbulent micro-channel flow under EDL effect reveals several questions. A transitional number of $Re_t = 817.5$, corresponding to $\kappa = 16.4$ of the reference case, would result in a half height channel in wall units (i.e., scaled by the shear velocity and viscosity) of $a^+ \approx 30$ in a low-Reynolds number fully developed turbulent microchannel flow. Recalling that the logarithmic equilibrium layer begins at 30 in wall units in macro-scale conventional turbulent channel flows, raises the question of the structure of “micro-turbulence” in such situations. Direct Numerical Simulations are currently used to clarify these questions.

REFERENCES

1. Drazin P.G., Reid W.H., 1981 “Hydrodynamic stability” Cambridge Un. Press, Cambridge (Ch. 7 pp. 370-464).
2. Gad-el-Hak M., 1999 “The fluid mechanics of microdevices” J. Fluids Eng., 121, 5-33.
3. Grosch C.E., Salwen H., 1968 “The stability of steady and time-dependent plane Poiseuille flow” J. Fluid Mech. 34, 177-205.
4. Hunter, R.J., 1981 “Zeta potential in Colloid Science” Academic Press, London.
5. Itoh, N. 1974 “Spatial growth of finite wave disturbances in parallel and nearly parallel flows. Part 1. The theoretical analysis and the numerical results for plane Poiseuille flow” Trans. Japan Soc. Aero. Space Sci. 17, 160-174.
6. Kulinsky L., Wang Y., Ferrari M 1999 “Electroviscous effects in microchannels” Proceedings of SPIE, The International Society of Optical Engineering, volume 3606, pp. 158-168.
7. Liqing Ren, Weilin Qu, Dongqing Li, 2001 “Interfacial electrokinetic effects on liquid flow in microchannels” Int. J. Heat and Mass Transfer, 44, 3125-3134.
8. Lykelma J., Minor M., 1997 Colloids and Surfaces A, 140, 33, 1.
9. Mala G.M., Li D., Dale J.D. 1997 “Heat transfer and fluid flow in microchannels” Int. J. Heat and Mass Transfer, 40 (13), 3079-3088.
10. Orszag S.A. 1971 “Accurate solution of Orr-Sommerfeld stability equation” J. Fluid Mech. 50, 689-703
11. Peng, XF., Peterson, G.P., Wang, B.X., 1994 “Heat transfer characteristics of water flowing through microchannels” Experimental Heat transfer, 7, 265-283.
12. Rahman, M.M., Gui F., 1993a “Experimental measurements of fluid flow and heat transfer in microchannel cooling passages in a chip substrate” ASME EEP 4(2), 685-692.
13. Stuart J.T., 1960 “On the non-linear mechanics of wave disturbances in stable and unstable parallel flows. Part 1 The basic behaviour in plane Poiseuille flow” J. Fluid Mech., 9, pp. 353-370.
14. Tardu S., 2003 "Transferts thermiques dans les microcanaux" Traité EGEM, Tome 6 Ch. 6, Microfluidique, 36p., Hermès.
15. Von Kerczek, C.H. 1982 “The instability of oscillatory Poiseuille flow” J. Fluid Mech. , 116, 91-114
Weilin Q., Mala G.M., Dongqing L., 2000. “Pressure-driven water flows in trapezoidal silicon microchannels” Int. J. Heat and Mass Transfer, 43, 353-364.
16. Yang C., Li D. 1997 J. Colloid Interface Sci., 194, 95.
17. Yang C., Li D. 1998 Colloids and Surfaces A 143, 339.

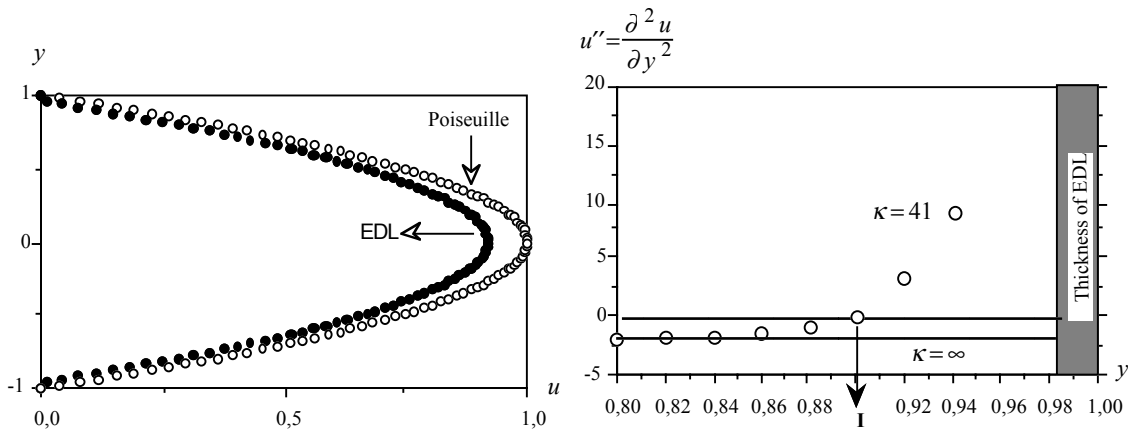


Figure 1 EDL and Poiseuille velocity profiles (a), and the inflexional instability of Fjortoft type (b). The parameters of the EDL flow are given in the text. The broken line in (b) corresponds to Poiseuille flow with $\kappa = \infty$ and the circles to the $\kappa = 41$ EDL flow. I shows the inflexion point The inviscid instability is of Fjortoft type.

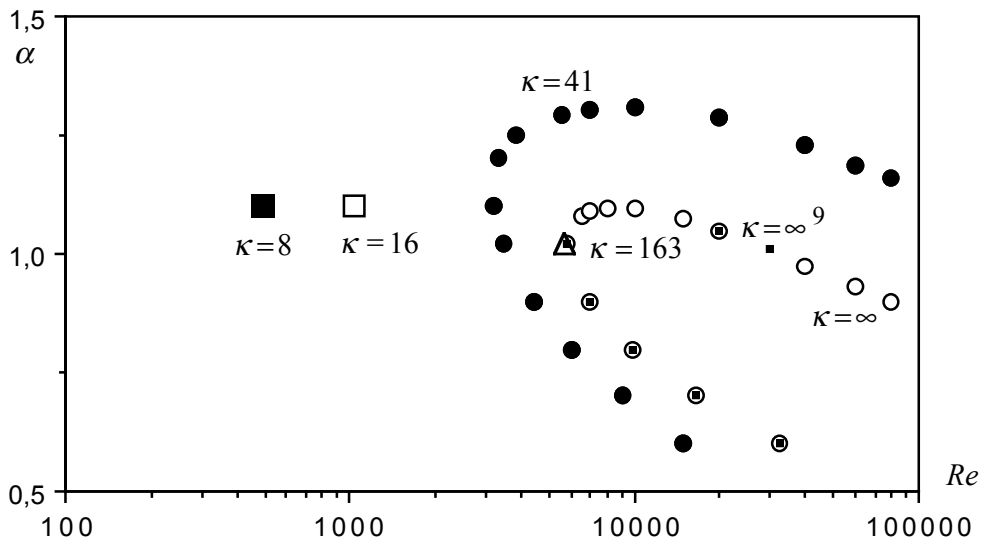


Figure 2 Neutral curves of the EDL flow compared with the Poiseuille flow. The open circles correspond to Poiseuille flow with $\kappa = \infty$. The results of Gresh and Salwen (1968) are shown by small bold squares. Bold circles correspond to $\kappa = 41, G = 12720$ and $\bar{\zeta} = 2.1254$. The rest of the results are obtained by changing the microchannel height and keeping constant the rest of the parameters.

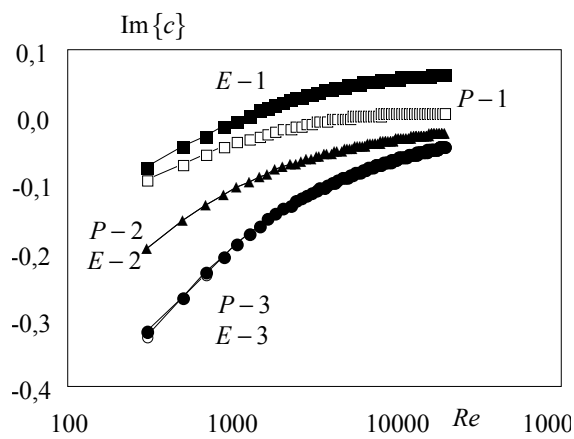
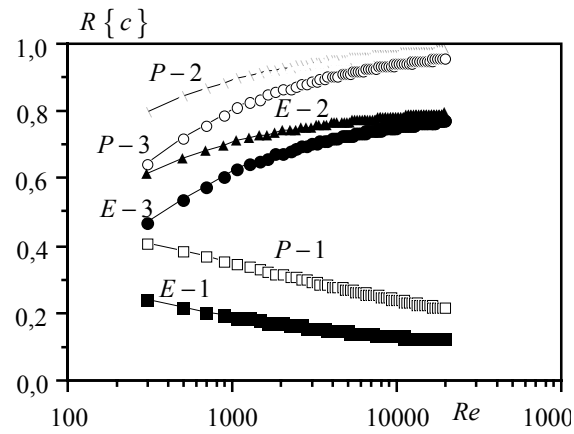


Figure 3 Real and imaginary parts (bottom) of the first three eigenvalues versus Re , $\alpha = 1$ and $\kappa = 16$.

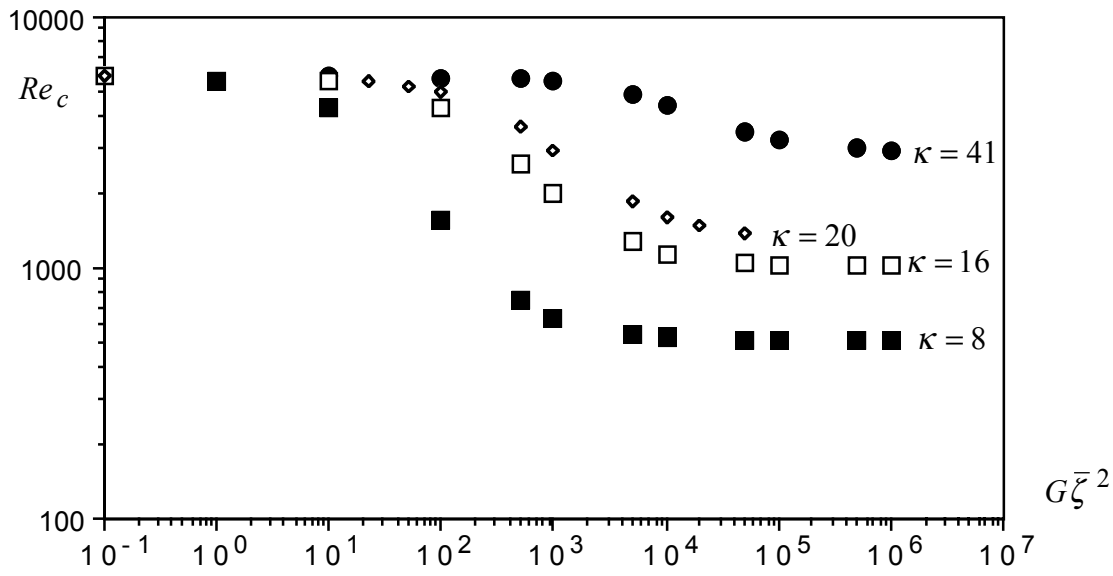


Figure 4 Distribution of the critical Reynolds number versus $G\bar{\zeta}^2$ for $\alpha=1.02$.

| κ | Range of $G\bar{\zeta}^2$ within Re_c decreases sharply Lower value-upper value |
|----------|--|
| 41 | $10^3 - 10^5$ |
| 20 | $10^2 - 10^4$ |
| 16.4 | $10^2 - 10^4$ |
| 8.2 | $10 - 10^3$ |

Table 1 Sensitivity of the critical Reynolds number to $G\bar{\zeta}^2$ variations.

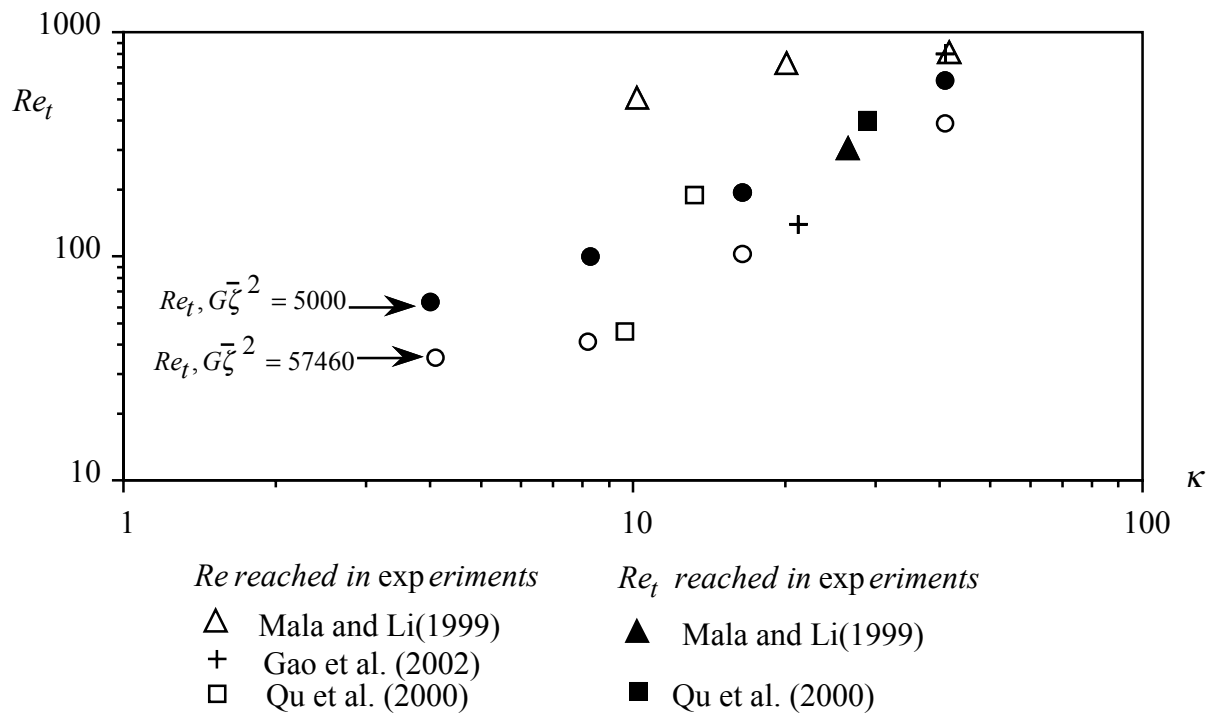


Figure 5 Estimated values of the transitional numbers under the EDL effect compared with some experiments and the range of Re numbers that can be reached in microchannels.